

# Meridional Energy Transport: Uncertainty in Zonal Means

David W. Keith

*Atmospheric Research Project, Harvard University  
12 Oxford St., Cambridge MA, 02138, USA.*

January 1994

## Abstract

The meridional energy transport in the atmosphere and ocean is computed using atmospheric analyses from ECMWF and NMC, and net radiative flux from ERBE. An error analysis of the zonally-averaged total transport shows that errors of  $\pm 7 \text{ Wm}^{-2}$  in net flux produce transport errors of  $\pm 0.5 \text{ PW}$  at the equator, an error of  $\pm 9\%$  in midlatitudes. Methods for correcting the mass non-conservation in transports derived from operational analyses are discussed. The ECMWF and NMC analysis systems now show remarkably similar zonally-averaged total energy transports, with normalized RMS differences of only 11%, despite 23% differences in Hadley-cell transports. The implied oceanic transport is derived along with an error estimate, and it is found to be broadly consistent with more direct measures of oceanic transport. The energy transport in NCAR's CCM1 and CCM2 is computed and is found to be about 20% larger than observations.

## 1 Introduction

Despite the fundamental role of meridional energy transport in determining global climate, estimates of its zonally-averaged magnitude, and especially of the partitioning between atmospheric and oceanic components, remain surprisingly uncertain. The total atmosphere plus ocean meridional transport is relatively well known from measurements of net top-of-the-atmosphere radiative flux. Indeed, the distribution of energy transport with latitude is strongly constrained simply by geometrical considerations, blackbody radiation, and the mean planetary albedo (Stone, 1978). However, The par-

titioning of meridional transport between atmosphere and ocean is more uncertain.

Atmospheric energy transport has been estimated from rawinsonde data (Oort, 1983), by use of archived global analyses from operational centers such as the ECMWF (Michaud and Derome, 1991; Masuda, 1988), and from model-corrected rawinsonde data (Savijärvi, 1988). Direct estimates of the oceanic component are even more uncertain due to the lack of relevant observations. Perhaps the best estimate of oceanic transport at a single latitude is at  $24^\circ$  N by Bryden et al. (1991), who estimate a annual-mean northward flux of  $2.0 \pm 0.42$  PW. (The  $\pm 0.42$  is based on a root-sum-of-squares of the  $\pm 0.3$  PW error estimates in the Atlantic and Pacific). As Bryden et al. point out, this is incompatible with the recent estimates of Carissimo et al. (1985) who found a total transport of 5.4 PW at  $24^\circ$  N and used the Oort (1983) atmospheric transport estimate of 1.7 PW to get an implied oceanic transport of 3.7 PW.

For this study new estimates of atmospheric transport were derived from ECMWF and NMC operational analysis products. The two data-sets now give encouragingly similar estimates of seasonally and zonally averaged transports, with residual differences of  $\sim 11\%$ . In order to assess the credibility of these estimates we examine their consistency with ERBE measurements of net flux and various oceanic measurements.

Our focus here is on estimates of zonally-averaged transports and their uncertainty. Previous estimates of atmospheric and total transport have not estimated errors, which makes it difficult to conclude much from inter-comparisons such as that at  $24^\circ$  N. This paper is motivated by the conviction that assessing error, even if the assessment is based on ad hoc assumptions, is a necessary precondition for a meaningful test of the consistency of transport estimates.

Uncertainty about the true values of oceanic and atmospheric energy transports have lead to their dismissal as a tool for validating climate models. One of the few recent comparisons of meridional transport in atmospheric models with observations (Stone and Risbey, 1990) found discrepancies as large as 40%. Estimation of error in the observations allows more meaningful comparison with models.

## 2 Atmospheric energetics

In Eulerian coordinates the continuity equation for total atmospheric energy including latent heat and ignoring viscosity is,

$$\frac{\partial}{\partial t} \rho (C_V T + gz + Lq + \frac{1}{2} \mathbf{v} \cdot \mathbf{v}) + \nabla \cdot \rho \mathbf{v} (C_P T + gz + Lq + \frac{1}{2} \mathbf{v} \cdot \mathbf{v}) = \rho Q_N. \quad (1)$$

The specific heat at constant pressure,  $C_P$ , appears in the energy flux vector rather than  $C_V$  as in the energy density because of the pressure-velocity work term,  $p\mathbf{v}$ , in the energy flux which reduces to  $\rho \mathbf{v} R T$  for an ideal gas (Oort and Peixoto, 1983). The net heating rate  $Q_N$  is due to radiative heating plus a small contribution from thermal conduction. It may be written as the difference between  $Q_1$ , the thermodynamic diabatic heating rate which includes heating due to condensation, minus  $Q_2$  which is the heating by condensation. Henceforth we will ignore the kinetic energy terms which amount to only  $\sim 10^{-3}$  of the total. In Lagrangian coordinates  $Q_1$  and  $Q_2$  are given by,

$$Q_1 = C_P \left( \frac{dT}{dt} - \kappa \frac{T}{p} \frac{dp}{dt} \right), \quad \text{and} \quad Q_2 = -L \frac{dq}{dt},$$

and they are calculated in pressure coordinates using,

$$Q_1 = C_P \left( \frac{\partial T}{\partial t} + \mathbf{v}_p \cdot \nabla T + \omega \left( \frac{\partial T}{\partial p} - \kappa \frac{T}{p} \right) \right) \quad (2)$$

$$Q_2 = -L \left( \frac{\partial q}{\partial t} + \mathbf{v}_p \cdot \nabla q + \omega \frac{\partial q}{\partial p} \right). \quad (3)$$

Where  $\mathbf{v}_p$  is the velocity along pressure surfaces,  $\omega = \frac{dp}{dt}$ , and  $\kappa$  is the compressibility,  $R/C_P$ .

For time scales greater than a year the time derivative of atmospheric energy density is much less than the mean net heating rate so we may ignore changes in stored energy and approximate (1) as

$$\nabla \cdot T_A \approx \tilde{Q}_1 - \tilde{Q}_2 = F_{TA} - F_S. \quad (4)$$

In this equation, and henceforth, vertical integrals of energy transports are denoted by “ $T$ ”s, and vertical energy fluxes by “ $F$ ”s, other vertically integrated quantities are indicated by tildes. Here,  $T_A$  is the vertical integral of the atmospheric energy-transport density,  $\rho \mathbf{v}_p (C_P T + Lq + gz)$ ,  $F_{TA}$  is the

top-of-the-atmosphere radiative flux, and  $F_S$  is the net energy flux into the surface including sensible and latent heat as well as radiation. This continuity equation plays an organizing role in this study by allowing comparison of different observational methods for estimating energy transport.

It is useful and common to disaggregate the transport of a scalar into transports due to transient eddies, mean meridional flow, and stationary eddies. The relevant identity is,

$$[\overline{xv}] = \overline{[xv]} = \overline{[x'v']} + [\bar{x}][\bar{v}] + [\bar{x}^* \bar{v}^*], \quad (5)$$

where  $x$  is a scalar field and  $v$  is the meridional velocity. Primes and stars indicate deviations from time and zonal means respectively, e.g.,  $x' = x - \bar{x}$ , and  $x^* = x - [x]$ .

Some care is necessary when computing these components in time- or zonally-varying coordinates. For example, suppose we wish to compute moisture transport by stationary eddies and we are working on sigma levels. In discrete coordinates the instantaneous moisture flux per unit length at a level with thickness  $\Delta\sigma$  is  $\frac{1}{g}p_s\Delta\sigma qv$ , where  $p_s$  is the surface pressure. One might suppose that the stationary eddy flux was  $\frac{1}{g}\Delta\sigma[\bar{p}_s][\bar{q}^* \bar{v}^*]$ , but in fact it is  $\frac{1}{g}\Delta\sigma \left[ \left( \bar{q} - \frac{[q\bar{p}_s]}{[\bar{p}_s]} \right) \left( \bar{v} - \frac{[v\bar{p}_s]}{[\bar{p}_s]} \right) \bar{p}_s \right]$ . The first expression includes spurious latitudinal covariances between the level thickness and  $x$  or  $v$ . In general we must choose a disaggregation of  $[\overline{xv\alpha}]$ , where  $\alpha$  is the level thickness, in which the eddy terms are free from covariances of  $x$  or  $v$  with  $\alpha$ , and which reduces to the previous definition when  $\alpha$  is constant. This is accomplished by replacing the zonal and time means with their  $\alpha$ -weighted counterparts; e.g., for the time means,

$$\bar{x} \rightarrow \frac{\overline{x\alpha}}{\bar{\alpha}}, \quad \text{and} \quad x' \rightarrow x - \frac{\overline{x\alpha}}{\bar{\alpha}}.$$

This produces a new identity,

$$[\overline{xv\alpha}] = \left[ \overline{\left( x - \frac{\overline{x\alpha}}{\bar{\alpha}} \right) \left( v - \frac{\overline{v\alpha}}{\bar{\alpha}} \right) \alpha} \right] + \frac{[\overline{x\alpha}][\overline{v\alpha}]}{[\bar{\alpha}]} + \left[ \left( \bar{x} - \frac{[\overline{x\alpha}]}{[\bar{\alpha}]} \right) \left( \bar{v} - \frac{[\overline{v\alpha}]}{[\bar{\alpha}]} \right) \bar{\alpha} \right] \quad (6)$$

whose terms correspond to those in Equation 5, and which gives the same decomposition into eddy components in  $\alpha$ -coordinates as the previous identity does in Eulerian-coordinates.

### 3 Transports from operational analyses

Archived analyses from operational weather prediction centers are histories of the global atmospheric state with uniform discretization in space and time, which thus provide a convenient basis for calculation of transport climatology. However, analysis/forecast systems are optimized for accurate weather prediction rather than climate analysis, and so these data must be carefully interpreted. The key difficulty is that analyses are strongly influenced by the forecast model and the analysis system, so that frequent changes in either component may introduce spurious tendencies into the archived analyses. We first discuss some general properties of the NMC and ECMWF analyses used in this study.

The wind and surface-pressure fields do not satisfy the equation of continuity, and must be adjusted to do so before transports are computed (Trenberth, 1991; Boer, 1986). The simplest method is to adjust the velocity field by addition of an altitude independent constant to ensure that divergence of the vertically-integrated mass flux is zero (Masuda, 1988; Michaud and Derome, 1991). In this study we follow Trenberth in including the pressure derivative term in the continuity equation, although its contribution turned out to be negligible. The deviation from continuity may be expressed as a pressure tendency,  $\psi$ ,

$$\frac{\partial p_s}{\partial t} + \nabla \cdot \int_{p_0}^0 \mathbf{v}_\perp dp/g = \psi. \quad (7)$$

Requiring that  $\psi = 0$  for a corrected velocity field  $\mathbf{v}'$  determines the divergence of the height-independent velocity correction  $\mathbf{c}$ , so we may take  $\mathbf{c} = \nabla\chi$  where  $\chi$  is the solution to the Poisson equation  $\nabla^2\chi = \psi$ . The corrected velocity is then given by  $\mathbf{v}' = \mathbf{v} - \mathbf{c}$ .

A few general characteristics of all analysis/forecast systems are relevant for computation of zonally-averaged transports.

- Systematic errors which are induced by inadequate resolution of topography tend to occur as dipoles which are strongly filtered by zonal-averaging.
- Several problems conspire to make the effect of forecast-model physics on the analysis greatest in the tropics. Motions are more diabatic in the tropics, so biases in heating terms such as radiation or convection come to dominate the energy budget more quickly than they do in

the extra-tropics. The Rossby adjustment time ( $f^{-1}$ ) is longer in the tropics, and the motion is less geostrophic, so observations of the mass field at a given spatial and temporal frequency constrain winds less strongly. Finally, observing systems make errors in wind speed which are roughly independent of latitude, but because the absolute magnitudes are less in the tropics the relative errors are larger.

- Although the Hadley cell strength is weakly determined by observations, there is less uncertainty in the total energy transport, due to a partial cancellation of the oppositely directed transports of dry static energy and latent heat. The energy flux is  $\rho\mathbf{v}$  times the moist static energy density ( $C_P T + gz + Lq$ ), and due to mass conservation, the zonally-averaged vertical integral of  $\rho\mathbf{v}$  is very small. Therefore, to the extent that moist static energy density is independent of height, the meridional energy transport is small. In reality, the upper tropical troposphere has mean relative humidity well below 50% which allows the upper level  $C_P T + gz$  transport to the winter hemisphere to dominate the reversed  $Lq$  transport at lower levels. Indeed, one may think of the system as “needing” to dry out the upper levels in order to achieve energy transport and so reduce the seasonal temperature gradients. Thus, although the analyzed Hadley-cell and hydrological cycle strength are strongly influenced by changes in analysis/forecast model-physics, the total energy transport is more robust due to cancellation of changes in moist and dry transports.
- Because it is almost uncorrelated with T or q the mass flux correction has little effect on the transport by transient eddies, and thus has little effect poleward of  $\sim 30^\circ$ .

### 3.1 ECMWF

Many previous studies have used ECMWF analyses to investigate atmospheric energetics. The FGGE IIIb analysis was used by Masuda (1988) to compute zonally-averaged energy transports, and by Fortelius and Holopainen (1990) to study diabatic heating rates and implied surface fluxes. Michaud and Derome (1991) studied zonally-averaged transports for the period 1981 to '86 focusing on '86. Trenberth and Olson (1988) compared NMC and ECMWF analysis over the period 1980 to '86 demonstrating significant systematic differences, as well as the strong effect of changes in ECMWF model physics on the analyses.

Since 1986, the last year examined by Michaud and Derome, the ECMWF analysis/forecast system has undergone significant changes, most importantly the new model physics of May '89 which include a new convection scheme and substantial changes to the parameterizations of radiation and gravity-wave drag. (The changes are cataloged in Trenberth (1992), page 9.) Interest in characterizing the effect of these system changes, along with the possibility of comparison with recent NMC analyses provided a partial motivation for this study.

The data used here are from the WCRP/TOGA archives I and II on the NCAR mass store (Trenberth, 1992), which are respectively 2 and 4 times daily uninitialized data on 14 pressure levels (15 after 1992). Both data sets are T42-truncated gridded data, from T106 spherical harmonics and 2.5° gridded data respectively.

Before transports were calculated, continuity was restored using the methods of Equation 7. The seasonally-averaged zonal mass flux was  $\sim 5 \times 10^{12} \text{ kg s}^{-1}$  before correction. The spatial average of time-RMS contribution of the  $\frac{\partial p}{\partial t}$  term in Equation 7 was typically only  $\sim 5\%$  of the total. Figure 1 shows transports for the period 1990-92.

Pressure level data is generated at ECMWF by interpolation from the model's hybrid coordinates. The interpolation is performed independently for each variable, which introduces significant imbalances in the mass flux. Since the interpolation of velocity is linear in the velocity, it seems likely that part of the mass-conservation error is proportional to velocity. In an attempt to correct this error an alternative mass flux correction method was tested on the ECMWF data. The vertically-integrated mass-flux correction was first determined by the methods of Equation 7; the vector mass-flux correction was then distributed between pressure levels proportional to horizontal speed and level thickness, resulting in a velocity correction proportional to horizontal wind speed. The differences between seasonal-mean zonally-averaged energy fluxes computed with velocity dependent and independent mass-flux corrections were of order 2% RMS. (Here and throughout, the RMS difference between two functions of latitude is the root of the mean-over-latitude of their squared difference. The RMS difference may be normalized by the root of the mean-over-latitude of  $\frac{1}{2}$  the sum of the squared functions.) This shows that errors in zonally-averaged fluxes are not much influenced by choice of mass-flux correction method, and thus the total error introduced by mass-flux correction is probably small.

All of the transport data presented were calculated from the horizontal energy flux which is independent of the vertical velocity field. It's also

possible to derive the transport from diabatic heating rates computed using Equations 2 and 3 which depend on the vertical velocities. If the vertical and horizontal velocities satisfied three-dimensional continuity then the divergence of the vertically-integrated horizontal transport would be equal to the vertical integral of the diabatic heating rate when energy storage terms were neglected. This is the approximate equality of Equation 4. In practice, the divergence of vertically-integrated moisture transport is nearly equal to  $-\tilde{Q}_2$ , with residual differences of  $\sim\%10$  in annual and zonal means. The errors in the dry-static energy budget are considerably larger.

Ehrendorfer et al. (1994) have recently demonstrated a variational method which adjusts the three-dimensional mass flux to ensure continuity while minimizing (in a least squares sense) changes in the individual velocity components. When they applied their method to ECMWF pressure-level data similar to that used in this study, they found that vertical velocity field required the largest relative corrections, and that horizontal velocity corrections increased with altitude. This is consistent with the smaller discrepancy between horizontal transport and diabatic heating rate found in the moisture budget ( $Q_2$ ), which samples only the lower atmosphere, and  $Q_1$ .

The mass flux correction scheme employed here modifies only the horizontal divergent velocities and ensures continuity only in a vertically-integrated sense. Diabatic heating rates were computed only as a measure of uncertainty. This choice was motivated by three factors; simplicity, consistency of application to NMC data for which vertical velocity was not available, and the assumption that the largest errors are in the vertical velocity field.

Although the errors introduced by choice of mass-flux correction are small, it is not clear that the errors introduced by interpolation to pressure surfaces are small. Indeed, the discrepancy between the diabatic heating rates and the horizontal flux divergence is evidence that significant uncertainty is introduced by the process.

ECMWF archives for the period December '85 to November '92 were analyzed to investigate changes of seasonal and annual transports over time. The annually-averaged total energy transport showed a small year-to-year variance of about 0.2 PW on peak transports of 4 PW. However, the annual transports had a strong secular trend in the southern hemisphere. In the mid 1980's the analysis showed asymmetric annual transport, with a northward transport of 4 PW at 40°N and -5 PW at 40°S. The magnitude of the Southern hemisphere transport decreased steadily during the late 1980's to -4.2 PW by '90, after which the analysis system showed roughly symmetric transports. The most important component contributing to the change in



total southern hemisphere transport was a decrease in the amount of dry static energy carried southward during the southern-hemisphere summer by the ascending arm of the Hadley cell. These changes are almost certainly due to changes in analysis system and model physics, most importantly the physics changes introduced in May '89.

### 3.2 NMC

Atmospheric analyses from NMC have not seen much use as a basis for transport calculations, possibly as a result of the differences between NMC and ECMWF analysis found by Trenberth and Olson (1988), who noted significant deficiencies in the southern hemisphere. A goal of this study was to determine if the new analysis system introduced at NMC in June '91 had resolved this discrepancy. The new system (Derber et al., 1991) features interpolation to global functions in model coordinates (sigma levels and spectral expansions), and includes methods to permit direct inclusion of heterogeneous observations such as satellite radiances. Along with the analysis system a new forecast model was introduced in March '91 which included an increase in horizontal resolution to T126 and changes in treatment of topography, stratus clouds and sea surface temperatures.

NMC data for the year beginning September '91 were analyzed using methods similar to those used for the ECMWF data. The data is available four times daily as virtual-temperature, divergence, vorticity, and specific-humidity on 18 sigma levels as grid-point data from the NMC T126 spectral model. Before processing, the data was transformed to a 128 by 64 - T42 truncation, and missing time periods which amounted to less than three days in total, were generated by filling from neighboring times.

In both the ECMWF and NMC data sets the failure to satisfy continuity is primarily caused by interpolation from model coordinates to the reduced grid of the analysis archive. Kevin Trenberth has found that it is best to interpolate to pressure surfaces before spatial truncation as the truncation in terrain-following coordinates is ill-defined. In this study, the seasonally and zonally averaged mass flux in the NMC sigma-level data was about three times smaller than found in the ECMWF analyses which had been interpolated to pressure levels.

### 3.3 Comparing the analyses

Transports derived from NMC and ECMWF analyses for the year beginning September '91 are shown in Figure 2, and are seen to be in remarkably good agreement. The annually-averaged transports of total energy differ by less than 11% RMS. As expected the agreement is best for the transient eddy transports which are less affected by model physics. The largest disagreement is seen in the transports of latent and dry static energy by the mean meridional circulation during the summer and winter seasons where the ECMWF estimates are about 30% larger than NMC's. This discrepancy is due to differences in Hadley cell strength which are also seen directly in the stream-functions. Transport of total moist static energy is less affected by differences in Hadley cell strength because of the near cancellation of the low-level transport of latent and sensible heat to the summer hemisphere and the upper-level transport of potential energy and sensible heat to the winter hemisphere.

The small inter-annual variability ( $\sim 5\%$ ) in zonally-averaged meridional energy transport implies that statistical errors are negligible in transport estimates based on data sets as short as two or three years. Almost certainly the dominant uncertainty is systematic error caused by deficiencies in data gathering and in the analysis/forecast systems. A *lower* bound on the systematic error is provided by the 11% RMS difference between NMC and ECMWF analyses. We know that uncertainty due to analysis method is at least this large. Changes in transport estimates due to previous analysis/forecast system changes provide another guide to the magnitude of the residual systematics. The May '89 changes at ECMWF which involved substantially new model physics and included a completely revised moist convection scheme, resulted in a 24% change in transport of latent heat by the Hadley-cell, yet only changed the zonally-averaged total energy transport by 10%. For the purpose of estimating errors in residual ocean transports we make the ad hoc assumption that the remaining error in atmospheric transports is  $\pm 15\%$  RMS in the zonal and annual means. This is quite probably an over estimate in the northern hemisphere mid-latitudes, and a less conservative estimate in the southern hemisphere.

An encouraging test of the internal consistency of the atmospheric observations is provided by the annual hydrological cycle shown in Figure 3B for ECMWF. As it should be,  $E - P$  is rarely positive over land. The NMC observations for 1991-92 show a similar quality in this respect, though as seen in Figure 2, the overall strength of the hydrological cycle is about 25%

smaller.

### 3.4 Analysis Systems *vs* Rawinsonde Networks

The atmospheric energy transports derived above are about 30% larger than those found by Oort (1983) based on interpolation from a rawinsonde network. It would be natural to ascribe the difference to inadequate spatial distribution of the rawinsondes. However, the discrepancy is of the same magnitude in the data rich northern midlatitudes as in the data sparse southern hemisphere. In addition, Oort (1978) investigated the effects of the spatial distribution of rawinsondes on transport calculations by simulating his analysis procedure on climate model output for which the “true” transports are known. He concluded that the spatial sampling was adequate to resolve the large scale circulation at issue here.

One may expect the analysis systems to give more accurate transport estimates because they incorporate more data, use known physical constraints, and, as will be shown in Section 3.3 produce results that are consistent with satellite and oceanographic observations. However, given that the root cause of this systematic discrepancy is unclear, and noting the simplicity and robustness of Oort’s methodology, one should be cautious about assuming that the analysis systems are giving the correct answer.

## 4 Consistency of ERBE, atmospheric, and oceanic observations

The difference between the atmospheric energy flux divergence and the net top of the atmosphere radiative flux is the energy flux into the surface:  $F_{TA} - \nabla \cdot T_A = F_S$  (Equation 4). Over land  $F_S$  must be near zero for times longer than a few months because of its low heat capacity. The deviation of  $F_S$  from zero provides a stringent test of the credibility of combined ERBE and atmospheric data. Additionally, one can compute oceanic energy transports using  $F_S$  over oceans and compare it with oceanographic observations.

Measurements of  $F_{TA}$  are available from the Earth Radiation Budget Experiment (ERBE) of the period December ’85 to ’89. Thus, there are two possibilities for estimating oceanic energy transport from ERBE data and ECMWF analyses. We may use ECMWF data from the same period as ERBE thus reducing the spurious effects of interannual variability on the implied ocean transport, or we may use the most recent ECMWF data pre-

suming that it is the most accurate, and that interannual variability is small enough to ignore. As discussed above, substantial changes in ECMWF’s analysis system during the late ’80s changed the zonal-mean southern hemisphere transports by  $\sim 20\%$ ; a change which swamps the apparent interannual variability of  $\sim 5\%$ . It thus appears that combining the most recent atmospheric analysis with the ERBE data offers the best hope for accurate estimates of zonally-averaged meridional oceanic transport. In a related study of ECMWF and NMC analyses in progress at NCAR, Kevin Trenberth and Amy Solomon have focused on the local energy budget, and so chose to look at the last year for which ERBE data were available. Although the close agreement between recent ECMWF and NMC analysis proves nothing, it lends credence to the assumption that the recent ECMWF analysis are more accurate than those of the late ’80s.

These difficulties serve to emphasize the importance of the reanalysis efforts at NMC and ECMWF which will consistently apply modern versions of the analysis/forecast algorithms to long time sequences of atmospheric observations. The questions raised above about the systematic error introduced by the interpolation to pressure levels imply that such reanalysis efforts would be most useful for transport calculations if results were saved daily in model coordinates.

#### 4.1 Meridional transport from ERBE data

Satellite measurements of net radiative flux have been used to estimate the meridional energy transport by atmosphere and ocean combined (Carissimo et al., 1985; Hartmann et al., 1986). However, there has been little effort to systematically estimate the effect of errors in satellite radiances on the transport estimates.

The transport is computed from the meridional continuity equation,

$$\frac{\partial T_T}{\partial \phi} = 2\pi a^2 \cos \phi (F_{TA} - \dot{E}), \quad (8)$$

by integration of  $F_{TA} - \dot{E}$  which by definition has a global mean of zero.  $\dot{E}$  is the time derivative of stored energy, and for the rest of this section transports and fluxes are considered as zonal-averages. Satellites measure  $F_{TA}$  with some error from which we must estimate  $F_{TA} - \dot{E}$  and error. We first consider  $F_{TA} - \dot{E}$ .

The ERBE data used in this study are an annual mean derived from the monthly climatology compiled by Hurrell and Campbell (1992) using

the S-4 data product for the period February '85 to December '88.  $F_{TA}$  has an area-weighted mean of  $8.4 \text{ Wm}^{-2}$ , which is about an order of magnitude larger than is physically plausible for a three year mean of  $\dot{E}$  given the thermal inertia of the oceanic mixed-layer and the constancy of oceanic temperatures. Thus the mean error in  $F_{TA}$  must be about this large.

Barkstrom and Smith (1986) estimate errors in ERBE data averaged over  $10^\circ$  zonal means of  $\pm 5 \text{ Wm}^{-2}$  in both the short-wave and long-wave components. Recent estimates of the errors have been made by Rieland and Raschke (1991) who suggest a global RMS error in seasonally averaged ERBE net radiation of  $7.8 \text{ Wm}^{-2}$  on  $2.5^\circ$  squares, most of which they attribute to error in the short-wave fluxes. Based on these estimates, and the mean error discussed above, a zonal RMS error of  $7 \text{ Wm}^{-2}$  in the three year average is assumed in the following error analysis.

Given the uncertainty expressed by the ERBE science team about the location of the mean error, it seems prudent to adopt the simplest method for correcting  $F_{TA} - \dot{E}$ : assume  $\dot{E}$  is zero and correct  $F_{TA}$  by subtracting its global mean.

An alternative method for deriving transports from fluxes is method "C" of Carissimo et al. (1985). Estimates of the transport are computed by integrating the uncorrected flux starting at the north and south poles, these transports  $T_{NP}$  and  $T_{SP}$  differ by a constant equal to the global integral of  $F_{TA}$ . The transport estimate is then constructed as the weighted sum of  $T_{NP}$  and  $T_{SP}$  with weight at each latitude inversely proportional to the distance from the respective poles; i.e.,  $T(\phi) = \frac{\phi+\pi}{2\pi}T_{NP}(\phi) + \frac{\pi-\phi}{2\pi}T_{SP}(\phi)$ . This method suffers from the disadvantage that there is no physically-realistic flux which corresponds to the estimated transport because  $\frac{1}{\cos\phi} \frac{\partial T}{\partial \phi}$  is unbounded at the poles.

In order to estimate the uncertainty in transport induced by error in  $F_{TA} - \dot{E}$  we construct an error function  $F_e$  which is a zonally-symmetric function with zero global mean and zonal RMS value  $\epsilon_{RMS}$ . The error in the flux may then be expressed as a sum of Legendre polynomials with uncertain coefficients  $\epsilon_n$ .

$$F_e(\mu) = \sum_{n=1}^{\infty} \epsilon_n P_n(\mu) \quad \text{with} \quad \sum_{n=1}^{\infty} \epsilon_n^2 = \epsilon_{RMS}^2. \quad (9)$$

where the  $P_n(\mu)$  are the normalized Legendre polynomials for  $\mu = \sin\phi$ . The resulting RMS error induced in the transport is the sum of the errors

induced by each wavenumber which are statistically independent.

$$T_e^2(\mu) = \sum_{n=1}^{\infty} \epsilon_n^2 \left( 2\pi a^2 \int_{-1}^{\mu} P_n(x) dx \right)^2 \quad (10)$$

The transport error function thus depends on the spatial power spectrum of the flux errors. The flux error is known to be systematic so we may assume that the error amplitude is concentrated at the large spatial scales, a reasonable choice is a  $1/f$  amplitude spectra:  $\epsilon_n^2 \propto \epsilon_{RMS}^2 (1/n^2)$ . Because the amplitude of the  $\int P_n$  functions decrease as  $1/n$  the series in equation 10 converges rapidly for any function  $\epsilon_n^2$  which decreases faster than  $1/n$ . The transport error function generated is insensitive to the choice of error power spectra and is dominated by the anti-symmetric  $P_1$  flux error. However, it is more likely that most of the ERBE error is symmetric about the poles; i.e., more  $P_2$  than  $P_1$ . We therefore make the arbitrary choice  $\epsilon_1^2 = 1/2\epsilon_2^2$  while maintaining the normalization of Equation 9.

With these choices for the power spectrum of the RMS flux error the transport error function  $T_e$  is given by,

$$T_e = 2\pi a^2 \epsilon_{RMS} \sqrt{0.0809 + 0.0441 \mu^2 - 0.378 \mu^4 + 0.629 \mu^6 - 0.702 \mu^8 + 0.326 \mu^{10}} \quad (11)$$

Total meridional energy transport and errors calculated by these methods are combined in Figure 4.

## 4.2 Implied oceanic energy transport

Previous studies have calculated the ocean transports as a residual by subtracting the zonal-average atmospheric transport from the total radiation derived transport (Michaud and Derome 1991; Masuda 1988; Oort 1983). A better method is to compute the residual transport over the oceans by integrating the implied surface flux,  $F_S$ ,

$$T_O(\theta) = a^2 \int_{\pi/2}^{\theta} \int_0^{2\pi} F_S \mathcal{O} \cos(\theta) d\lambda d\theta \quad (12)$$

where  $\mathcal{O}$  is a ocean-only masking function. This method should give a more accurate estimate of  $T_O$ , and more importantly, allows estimation of error by calculating the implied “land transport.”

Before computing the ocean transport, the surface flux is adjusted by addition of a constant which ensures that the integral of  $F_S$  over the oceans

is zero. The required adjustment flux is a measure of the mean error in  $F_S$  which may be used to estimate the errors in the ocean transports using the methods outlined above.

It's difficult to assess the errors in the implied oceanic transport. The methods of the previous section are not strictly applicable because the flux error function is constrained by the requirement that its integral be zero over the oceans rather than over a sphere. In any case it is unclear how to assess the RMS uncertainty in  $F_S$ . A plausible approach is to assume that the errors in ERBE total transport and in the atmospheric transport are uncorrelated, and then to add them quadratically using error estimates from sections 3.1 and 2.3 respectively. Error estimates made by this method along with the total oceanic transport using ECMWF data from the years 1991-92 are shown in Figure 5.

The oceanic transport can be disaggregated into components due to various basins by using a basin-specific masking function in Equation 12, Figure 6 shows the resulting transports. One could proceed farther still, and solve Poisson's equation to determine the divergent part of the vertically integrated vector heat transport, but the quality of the residual surface flux,  $F_S$ , discussed below, seems insufficient to justify this step.

If the error analysis presented here is correct, the residual method now puts as strong a constraint on oceanic transport as do oceanographic methods. There are several reasons to be cautious about this conclusion.

- Satellite radiance measurements are used by the operational analysis systems, so the assumption that their systematic errors are uncorrelated with ERBE data may be false.
- The attribution of systematic error to transports derived from analyses/forecast systems is fundamentally ad hoc.
- The differences between the transports derived from analysis/forecast systems and from rawinsondes have not yet been adequately resolved.

### 4.3 Consistency of observations

Comparing oceanic transports derived as residuals with various direct oceanographic measurements provides an overall assessment of the certainty of our understanding of meridional energy transport.

The implied surface energy flux permits a strong test of the quality of the combined atmospheric energy flux divergence and ERBE net radiation— $F_S$

over land should be zero to  $\sim 0.1\text{Wm}^{-2}$  in an annual average. Figure 3A shows  $F_S$  for the 1991-92 ECMWF data combined with the ERBE climatology. The results are discouraging.  $F_S$  departs significantly from zero, with errors which appear predominantly in the form of latitudinal dipoles centered on regions of steep topography. The cancellation of these dipoles explains why the zonal-average transports look so reasonable.

Direct measurement of oceanic transport is notoriously difficult. The Bryden et al. (1991) transects at  $24^\circ\text{N}$  in the Atlantic and Pacific represent perhaps the best determination of transport at a single latitude, they estimate errors of 21% on a total transport of 2 PW. Oceanic transport can be estimated using inverse methods given known distributions of tracers and their sources and sinks. A recent application of this method by Macdonald (1993) at  $30^\circ\text{S}$  resulted in an estimated heat transport of  $-0.7 \pm 0.1$  PW, and additionally contains an comprehensive review of southern hemisphere transport estimates.

As shown in Figures 5 and 6, the oceanic transports derived here by residual methods are consistent, within estimated errors, with the best oceanographic estimates. This agreement is considerably better than was found in previous studies. Carissimo et al. (1985) used the Oort rawinsonde data and combined it with early '80s satellite data to derive oceanic transports of 3.5 PW at  $24^\circ\text{N}$  and over 2 PW poleward in the southern hemisphere. These differences are explained by the  $\sim 1$  PW larger atmospheric transports found in this study combined with a 0.8 PW smaller estimate of total transport in the southern hemisphere. Michaud and Derome (1991) used '86 ECMWF analyses to derive a total atmospheric transport very similar to the results reported here. However, based on NIMBUS 7 ERB radiances they found oceanic transports of 3.2 PW at  $24^\circ\text{N}$  and  $\sim 1.5$  PW poleward between  $10^\circ\text{N}$  and  $50^\circ\text{S}$ .

## 5 Models

Stone and Risbey (1990) found an approximate factor of two over estimation of meridional energy transport in several of the climate models they examined, including GISS II, GFLD-R15, and NCAR's CCM0B, when compared with Oort's observations. This strong result provided significant motivation for the present work. Energy transports from two more recent NCAR models, CCM1 and CCM2, were computed using the methods described above (ignoring the unnecessary mass flux correction) and are shown in Figure



7. The agreement between models and observations now looks considerably better. Peak transports in CCM 1 and 2 are  $\sim 5$  PW, a bit smaller and more symmetric than the models which Stone and Risbey examined, and the ECMWF and NMC analyses presented here have peaks of  $\sim 4$  PW, about 1 PW higher than Oort's estimate. However, the model results were derived under incompatible conditions; CCM 1 and 2 were run with prescribed sea surface temperatures allowing implicit oceanic heat transport whereas CCM0B was run with a "swamp ocean" which permits no transport.

Based on the error analysis presented above, the remaining 20% disagreement between CCM 1 and 2 and the data can not be easily ascribed to observational uncertainty and thus represents a significant, though small, deficiency in the models.

## 6 Conclusions

An error analysis of the total energy transport derived from satellite radiance measurements shows that a  $\pm 7 \text{ Wm}^{-2}$  (one standard deviation) error in the net radiative flux implies an error in the meridional transport of  $\sim \pm 0.5$  PW at latitudes equatorward of  $45^\circ$ , which is a relative uncertainty of  $\pm 9\%$  at  $30^\circ$  N or S.

Estimation of errors in atmospheric transport derived from operational forecasting systems is more difficult. The similarity of energy transport in ECMWF and NMC analyses, which now have normalized RMS differences of 11%, is encouraging. In addition, the robustness of moist static energy transport under model-physics induced changes in Hadley-cell strength due to the cancellation of changes in moist and dry transport terms, increases confidence in the analyses. For the purpose of assessing uncertainty in residual ocean transport we assumed that the remaining error in meridional atmospheric transport is 15%, which is 50% larger than the changes in transport due to the May '89 physics changes at ECMWF, or the current ECMWF-NMC difference.

Ocean transport was computed using residual surface energy fluxes over oceans only. Its error was estimated by taking the root-sum-of-squares of the errors in the zonally averaged atmospheric and total transports. Under these assumptions the implied ocean transport has a peak of  $2.7 \pm 0.7$  PW at  $20^\circ$  N, a relative uncertainty of 22%. This oceanic transport estimate was found to be consistent with more direct measurements, although the agreement was considerably better in the Atlantic than in the North Pacific. For

example, the inconsistency in total transport at  $24^\circ$  N noted by Bryden et al. (1991) is resolved by the increase in atmospheric transport as compared to the Oort (1983) estimate. The compatibility of zonally-averaged atmospheric, oceanic, and total transports gives strong encouragement that recent transport estimates are getting closer to the truth.

The atmospheric transport derived here is about 30% larger than found by Oort (1983). However, the differences between the transport estimates are as large in the northern midlatitudes as in the southern hemisphere, making it hard to ascribe the discrepancy to inadequate spatial sampling in the rawinsonde based data. The cause of this discrepancy needs to be resolved before one can be fully confident in deriving transports from the analysis systems.

Agreement between observations and recent versions of Community Climate Model is considerably better than found by Stone and Risbey (1990) in their intercomparison. This is due to larger estimates of observed transport and smaller transports in CCM 1 and 2 which were run with fixed sea surface temperatures. However, it is unclear how to interpret this given the differing treatment of oceanic transport.

Although significant uncertainty remains in estimates of total meridional transport, and in its partition between oceanic and atmospheric components, the uncertainties are small enough that they should be used as a constraint on coupled ocean-atmosphere climate models many of which have transports which differ from these estimates by more than their errors.

## 7 Acknowledgments

This work benefited from discussions with Phil Rasch, Maurice Blackmon, Peter Stone, and Joe Tribbia. Kevin Trenberth provided invaluable criticism, and, along with Jeff Berry, helped me gain access to the data. I thank two anonymous referees for their thoughtful reviews. A special debt is owed James Risbey for encouraging my interest in these questions. NCAR's Scientific Computing Division provided computer time and access to the data sets. I thank ECMWF and NMC for allowing access to their data. Finally, I am grateful for support from the NOAA PostDoctoral Program in Climate and Global Change.

## References

- Barkstrom, B. R., and G. L. Smith, 1986: The earth radiation budget experiment: Science and Implementation. *Rev. Geophys.*, **24**, 379–390.
- Boer, G. J., 1986: A Comparison of Mass and Energy Budgets from Two FGGE Datasets and a GCM. *Mon. Wea. Rev.*, **114**, 885–902.
- Bryden, H. L., D. H. Roemmich and J. A. Church, 1991: Ocean heat transport across 24°N in the Pacific. *Deep-Sea Res.*, **38**, 297–324.
- Carissimo, B. C., A. H. Oort and T. H. Vonder Haar, 1985: Estimating the Meridional Energy Transports in the Atmosphere and Ocean. *J. Phys. Oceanogr.*, **15**, 82–91.
- Derber, J. C., D. F. Parrish and S. J. Lord, 1991: The new global operational analysis system at the National Meteorological Center. *Weather and Forecasting*, **6**, 538–547.
- Ehrendorfer, M., M. Hantel and Y. Yang, 1994: A variational modification algorithm for three-dimensional mass flux non-divergence. *Quart. J. Roy. Meteor. Soc.*, **120**, in press.
- Fortelius, C., and E. Holopainen, 1990: Comparison of Energy Source Estimates Derived from Atmospheric Circulation Data with Satellite Measurements of Net Radiation. *J. Climate*, **3**, 646–660.
- Hall, M. M., and H. L. Bryden, 1982: Direct estimates and mechanisms of ocean heat transport. *Deep-Sea Res.*, **29**, 339–359.
- Hartmann, D. L., V. Ramanathan, A. Berroir and G. E. Hunt, 1986: Earth radiation budget science. *Revs. Geophys. Space Phys.*, **24**, 439–468.
- Hurrell, J. W., and G. G. Campbell, 1992: Monthly Mean Global Satellite Data Sets Available in CCM History Tape Format. NCAR Tech. Note NCAR/TN-371+STR, National Center for Atmospheric Research, Boulder, Colo., 94 pp.
- Macdonald, A. M., 1993: Property fluxes at 30°S and their implications for the Pacific-Indian Throughflow and the Global Heat budget. *J. Geophys. Res.*, **98**, 6851–6868.
- Masuda, K., 1988: Meridional heat transport by the atmosphere and the ocean: analysis of FGGE data. *Tellus*, **40A**, 285–302.

- Michaud, R., and J. Derome, 1991: On the meridional transport of energy in the atmosphere and oceans as derived from six years of ECMWF analyses. *Tellus*, **43A**, 1–14.
- Oort, A. H., 1978: On the adequacy of the rawinsonde network for global circulation studies tested through numerical model output. *Mon. Wea. Rev.*, **106**, 174–195.
- Oort, A. H., 1983: Global Atmospheric Circulation Statistics, 1958–1973. NOAA Professional Paper 14, U.S. Government Printing Office, Washington, D. C., 180 pp.
- Oort, A. H., and J. P. Peixoto, 1983: Global Angular Momentum and Energy Balance Requirements from Observations. *Theory of Climate*, B. Saltzman, Ed., Vol. 25, Advances in Geophysics, 355–490.
- Rieland, M., and E. Raschke, 1991: Diurnal variability of the earth radiation budget: sampling requirements, time integration aspects and error estimates for the earth radiation budget experiment (ERBE). *Theor. Appl. Climatol.*, **44**, 9–24.
- Savijärvi, H. I., 1988: Global Energy and Moisture Budgets from Rawinsonde Data. *Mon. Wea. Rev.*, **116**, 417–430.
- Stone, P. H., 1978: Constraints on dynamical transports of energy on a spherical planet. *Dyn. Atmos. Oceans*, **2**, 123–139.
- Stone, P. H., and J. S. Risbey, 1990: On the Limitations of General Circulation Climate Models. *Geophys. Res. Lett.*, **17**, 2173–2176.
- Trenberth, K. E., 1991: Climate Diagnostics from Global Analyses: Conservation of Mass in ECMWF Analyses. *J. Climate*, **4**, 707–722.
- Trenberth, K. E., 1992: Global analyses from ECMWF and atlas of 1000 to 10 mb circulation statistics. NCAR Tech. Note, NCAR/TN-373+STR, National Center for Atmospheric Research, Boulder, Colo., 191 pp.
- Trenberth, K. E., and J. G. Olson, 1988: An evaluation and intercomparison of global analyses from NMC and ECMWF. *Bull. Amer. Meteor. Soc.*, **69**, 1047–1057.
- Wunch, C., 1984: An Eclectic Atlantic Ocean Circulation Model. Part I: The Meridional Flux of Heat. *J. Phys. Oceanogr.*, **14**, 1712–1733.

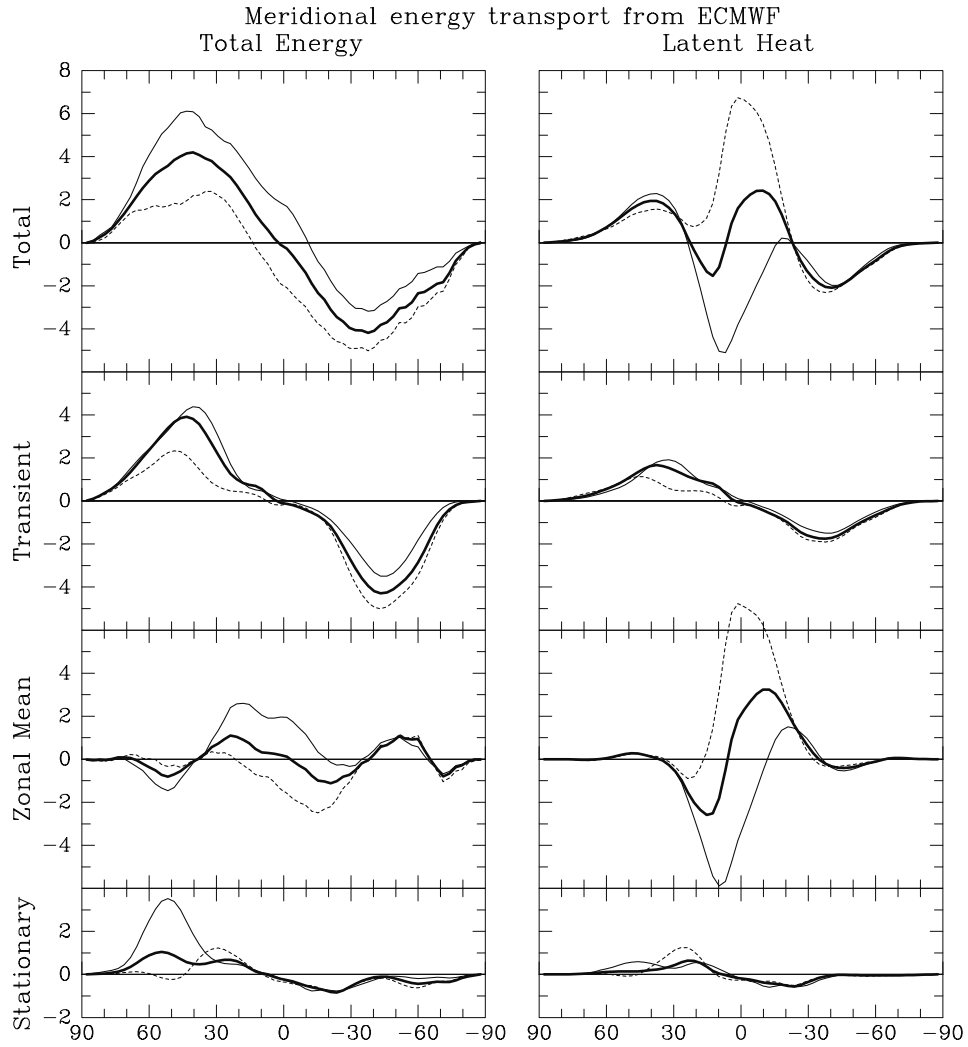


**Figure 1** Atmospheric meridional energy transports in PW ( $10^{15}$  W) from three years of ECMWF analyses beginning in September '89. The left column shows transports of total energy, the right of latent heat. The four plots stacked vertically show total transport, transport by transient eddies, mean meridional circulation, and zonal eddies respectively. In each case the thick line is annual mean, the thin line is December-January-February, and the dashed line is June-July-August.

Meridional energy transport from ECMWF and NMC

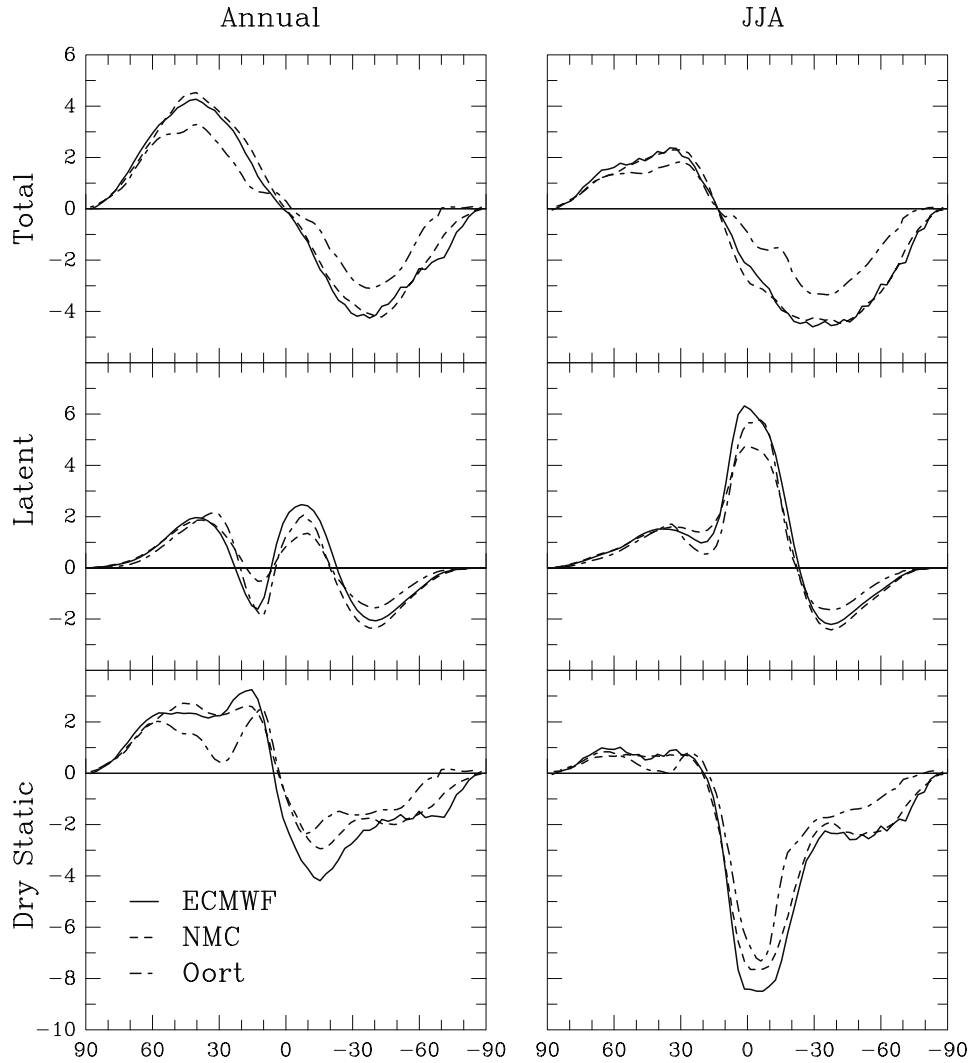


**Figure 2** Comparison of atmospheric energy transport computed from ECMWF and NMC global analyses for the period September '91 to August '92. The units of transport are PW ( $10^{15}$  W). The left column shows annual averages, the right is a June-July-August average which more clearly shows the Hadley cell differences. From the top the three plots stacked vertically show transports of total energy, latent heat, and dry static energy ( $C_p T + gz$ ). Values from the Oort (1983) data are shown for comparison.

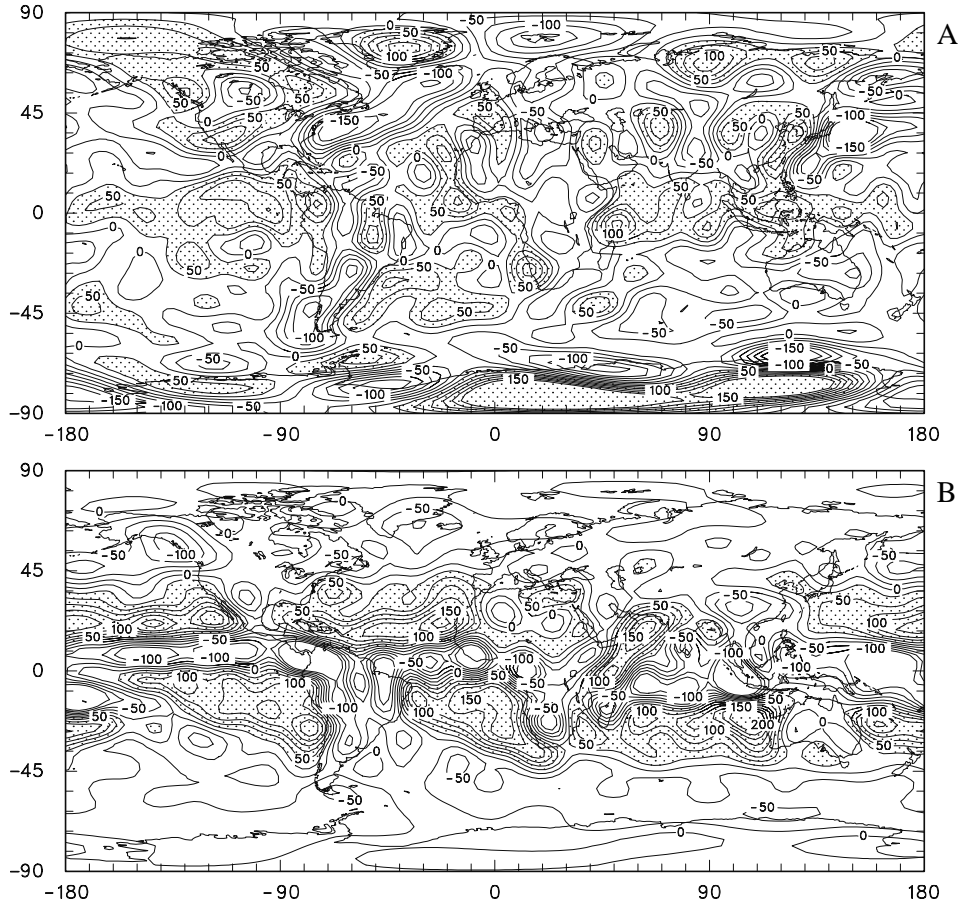


**Figure 3** Downward surface energy fluxes derived from ECMWF atmospheric analyses and ERBE data. In both plots the contour interval is  $25 \text{ Wm}^{-2}$ , values over  $25 \text{ Wm}^{-2}$  are stippled. The ECMWF data is a two year average of horizontal transport beginning in September '90. (A) The net downward surface energy flux,  $F_S = F_{TA} - \nabla \cdot T_A$  (see Equation 4). Where  $F_{TA}$  is from a normalized three-year mean of the ERBE S-4 data, and  $T_A$  is the horizontal transport. The  $F_S$  field has several obvious flaws; the surface flux should be zero over land, and the strong dipoles around prominent topographic features are clearly erroneous. Note the strong energy fluxes out of the ocean in the Gulf Stream and Kuroshio western boundary currents. (B) The divergence of vertically integrated horizontal moisture transport which is equivalent to  $-\bar{Q}_2$ , and proportional to  $E - P$ . ( $29 \text{ Wm}^{-2} = 1 \text{ mm day}^{-1}$ .)

Total energy transport and errors from ERBE

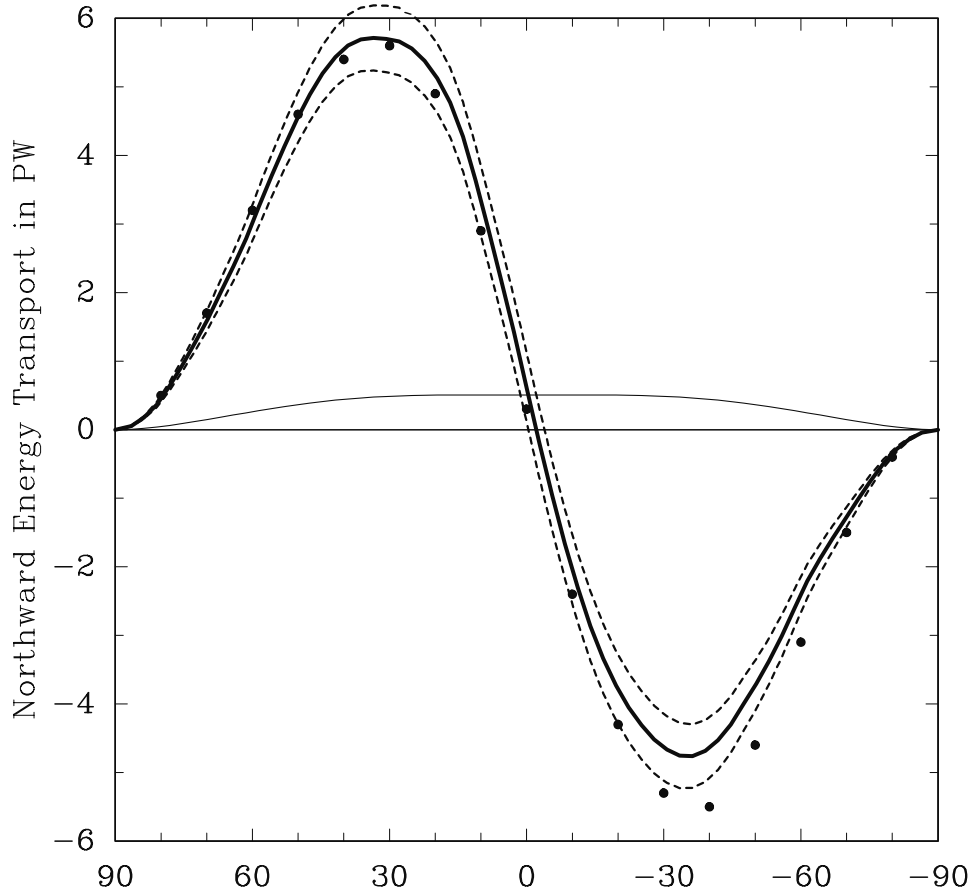


**Figure 4** Meridional transport of energy in the atmosphere-ocean system (Thick line) derived from top-of-the-atmosphere net radiative flux as determined by a three year mean of the ERBE S-4 data set. The dashed curves indicate uncertainty in the transport due to an assumed  $\pm 7 \text{ Wm}^{-2}$  ( $\epsilon_{RMS}$ ) systematic error in the zonally-averaged net radiation under the assumptions used in deriving Equation 11. The thin solid line shows the same error function plotted alone. The dots are data from Carissimo et al. (1985).



Residual Ocean Transport with Errors

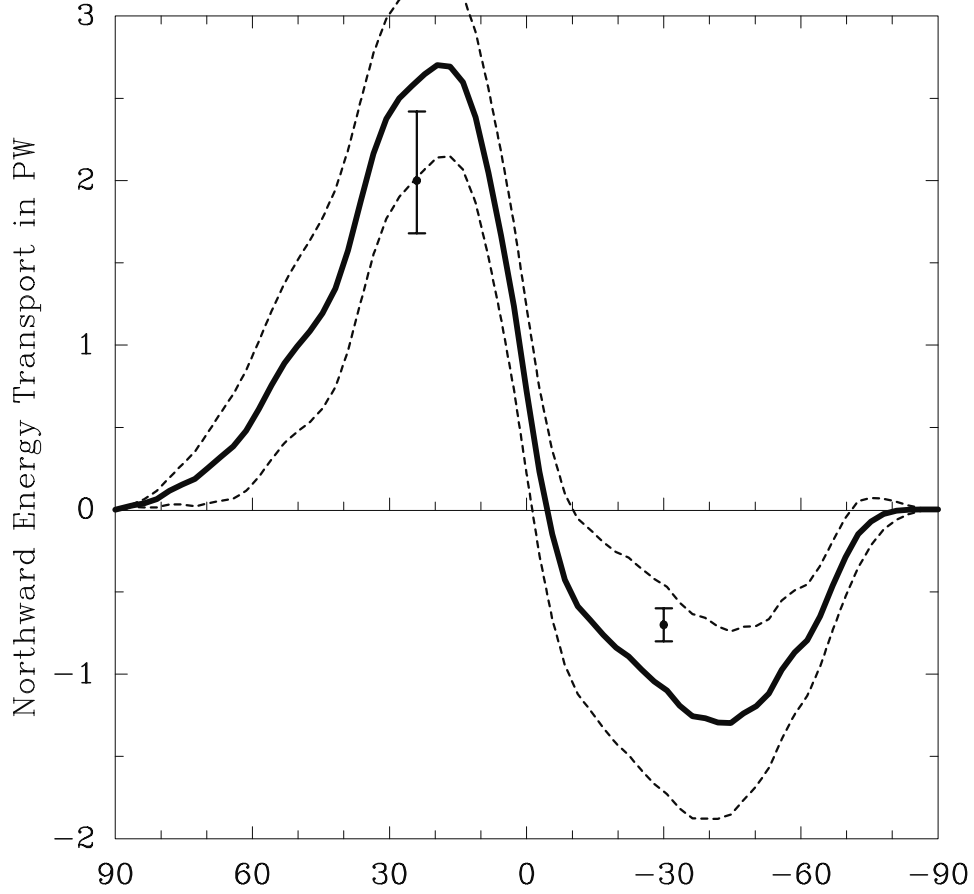


**Figure 5** Total oceanic energy transport with errors derived as a residual and compared with various direct estimates. The transport is computed by first adjusting the net surface energy flux,  $F_S$  (see Figure 3 and text), to be zero when integrated over the oceans, and then integrating from either pole. The “direct” estimates are from Bryden et al. (1991) at 24° N, and Macdonald (1993) at 30° S.

Residual Energy Transport in Atlantic and Indo-Pacific

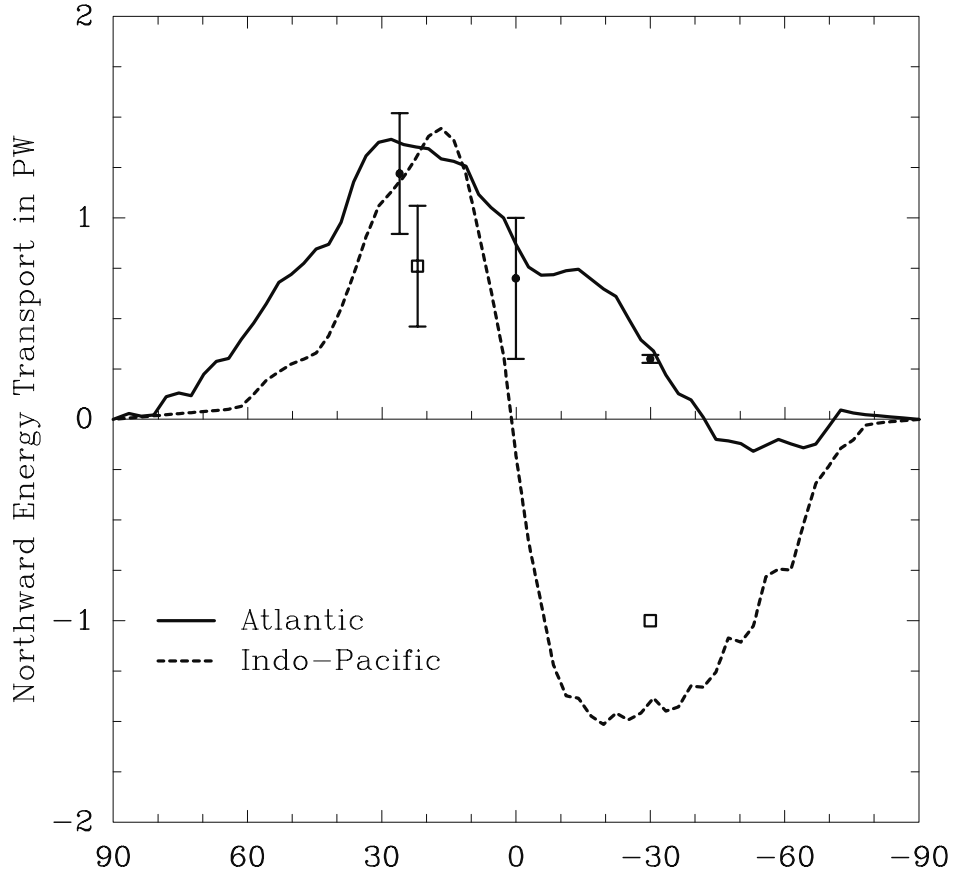


**Figure 6** Ocean transport in the Atlantic and Indo-Pacific basins. The solid dots and error-bars show estimates of Atlantic transport. From North to South they are; Hall and Bryden (1982), Wunch (1984), and Macdonald (1993). The open boxes are Indo-Pacific transports from Bryden et al. (1991) and Macdonald (1993).

Meridional energy transport from ECMWF, CCM1, and CCM2

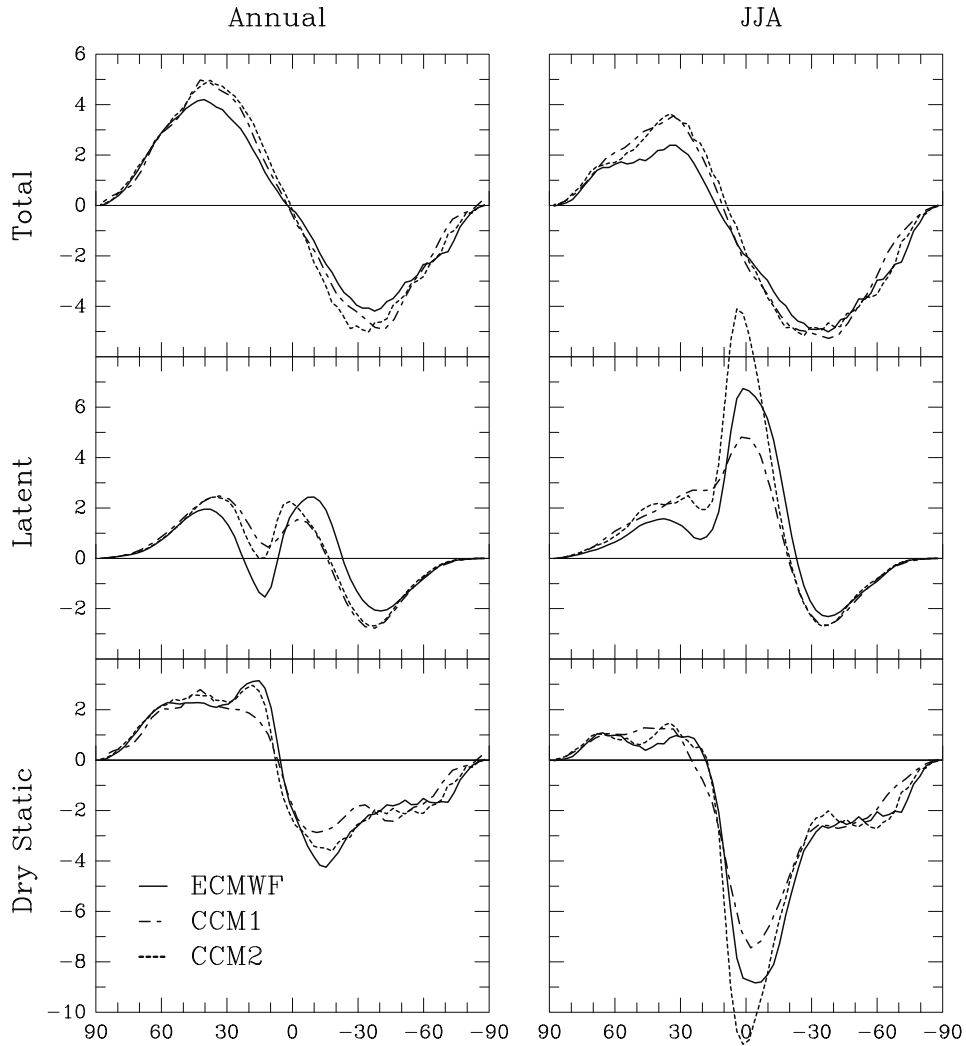


**Figure 7** Atmospheric energy transport in PW derived from three years of ECMWF analyses beginning in September '89, and compared with the climate models CCM1 and CCM2. As in Figure 2 the left column is annual average and the right is JJA, and the three plots stacked vertically show transports of total energy, latent heat, and dry static energy ( $C_P T + gz$ ) respectively.